Progress In Electromagnetics Research C, Vol. 125, 179–189, 2022

Elimination of Cogging Torque and Torque Ripple in Magnetic Gear Using Slicing Technique

Muhammed K. Rashid* **and Ahmed M. Mohammed**

Abstract—Magnetic gears (MGs) have many advantages over mechanical gears, including high efficiency, no contact, no lubrication, and low noise. Even though MGs are energy-efficient, cogging torque and torque ripple are always challenging, especially in low-speed applications. Generally, the cancellation of cogging torque enhances the performance of the operation of PM machines. This article proposes an approach based on slicing technique through which reduced cogging torque and improved torque density can be achieved in MGs. The two-dimensional finite element method (2D FEM) has been used to analyze the models using Simcenter and MATLAB software packages. The results show that the elimination of cogging torque of the proposed models compared to the base model is 97.53% on the inner rotor, and that of the outer rotor is 42.23%. Also, the torque density is slightly improved by 0.05% on the inner rotor while 0.1% improvement on the outer rotor is obtained.

1. INTRODUCTION

Recently, magnetic gears (MGs) have drawn much interest, especially in electric vehicles [1]. Multiple torque-dense MG approaches have been put out in the literature [2–4], including flux-modulated, harmonic, and planetary MGs. Due to its more straightforward mechanical design and flexibility in making a single volume of a magnetic geared electric machine, flux-modulated MG is the one that garners the most interest [5]. As seen in Fig. 1, an MG comprises three concentric parts: a flux modulator, an inner magnet arrangement peripherally mounted on an inner back iron, and an outer magnet arrangement with an outer back iron. The slotting effects of the modulator make the MGs susceptible to cogging torque, which are considered as the main contributor to the torque ripple [3, 6], just like any other traditional permanent magnet (PM) machine with a slotted stator [7].

Different studies for cogging torque mitigation approaches can be found in the literature. In [8], slicing technique has been used to mitigate the cogging torque of the inner rotor of MGs. In [9], two methods are proposed to mitigate the torque ripple in doubly salient PM machines; the first method developed a combination of stator and rotor teeth depending on the shapes and dimensions of the teeth, while the other method used the nonlinear indirect torque technique. Two new dissymmetric pole radial magnetic gears (RMGs) are proposed in [10, 11], where the PMs on the inner rotor are constructed from Halbach arrays with unmatched magnetic poles and irregular magnet configuration, improving the output torque and magnetic flux density. The basic geometrical structure of the rotor lamination of interior permanent magnet synchronous machines (IPMSMs) is progressively modified by [12] to give a simplified cogging torque minimization method. The authors in [13] proposed a method for axial flux permanent magnet (AFPM) machines in which the angle of PM placement is adjusted to obtain a reduced cogging torque. The loaf-shape PM for reducing cogging torque is suggested in [14]. The authors in [15] examined the effect of three strategies for reducing cogging torque: PM segmentation method, PM shifting method, and composite material PMs method. In [16], the authors investigated

Received 31 August 2022, Accepted 3 October 2022, Scheduled 17 October 2022
* Corresponding author: Muhammed Khudair Rashid (muhammed.k.alrikabi@uotechnology.edu.iq).
The authors are with the Department of Electrical Engineering, University of Technology, Baghdad 10066, Iraq.

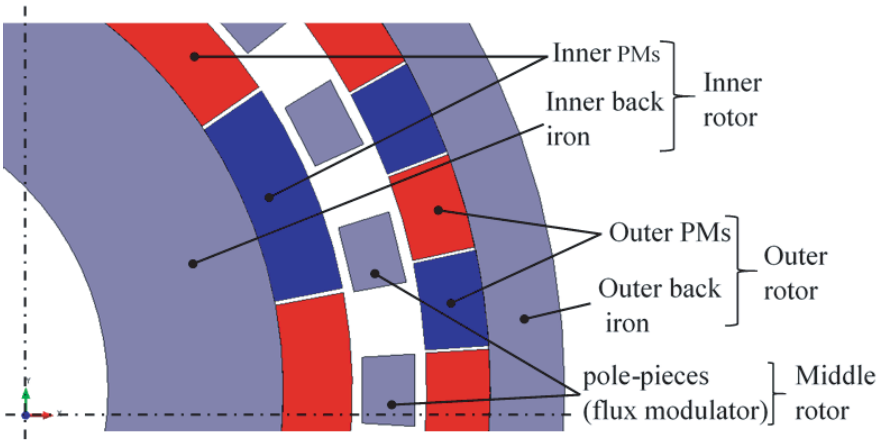

Figure 1. MG components.

the influence of various magnetization modes on the performance of the MG. In [17], several techniques for decreasing cogging torque for specific applications were investigated, such as PM segmentation, adding unique slots, and inlaying two-part rotors. Two enhanced step-skewing approaches are proposed and examined in [18]; rotor step-skewing with unequal step lengths and the rotor step-skewing with optimum skew angles, for the mitigation of cogging torque of the inner rotor of permanent magnet synchronous machines (PMSMs). A modulated pole machine with a high torque density has been introduced by [19]; this study developed a tooth pitching technique to overcome the issue of high cogging torque. Implementing a new combination of stator teeth and pole shoes to reduce cogging torque is suggested in [20]. In [21], a novel method for cogging torque mitigation has been proposed by generating a sinusoidal air gap flux density using Halbach arrays in coaxial magnetic gear (CMG). A sealed slot with a sliding separator has been proposed in [22] to mitigate the cogging torque. However, getting a slider into a slot on small machines is highly challenging. In [23], the authors suggested rotor notches as a cogging torque mitigation approach. [24] suggested a new approach for the winding side and coil winding which effectively reduces cogging torque and makes the winding more difficult.

From the literature perspectives, slicing one rotor of MG reduces the cogging torque of one rotor, while the cogging torque of the other rotor will not be reduced. Rotor notches mitigate the cogging torque at the expense of the useful torque. The tooth pitching technique reduces the cogging torque in large PM machines with the cost of a small reduction in the rated torque. Skewing the rotor reduces the cogging torque efficiently, but the significant reduction in the torque is the main disadvantage. The construction of magnets of the rotor with Halbach array makes the PM machines have efficient performance through which both the elimination of cogging torque and improvement of the torque are obtained, but the complexity in the magnets manufacturing is increased.

In this work, a cogging torque minimization method is introduced and analyzed using slicing method for both rotors of the MG. This method is efficient in reducing the cogging torque of PM machines and the condition upon which the method is applied. A slice (say the second slice) is shifted angularly from the first slice by an appropriate angle, and the third slice is shifted from the second slice by the same angle and so on. In other words, the third slice is shifted from the first slice by doubled angle, and the angle of shifting is determined depending on the number of slices and the cogging torque cycle, as it will be discussed in the next sections. In addition to the satisfying results in mitigating the cogging torque, the slicing technique improves the torque density. Also, the size of magnets in each slice is smaller than that of the unsliced magnets, so the feasibility of maintenance of each slice separately is high. However, this method requires the high accuracy of rotor machining.

2. BASICS OF COGGING TORQUE

For PM machines, the cogging torque is load-independent resulting from the interaction between the PMs of the rotor and the structure of slotted iron, which can be expressed as in (1) [6]

$$T_{cog} = -\frac{1}{2}\varphi^2 \frac{dR}{d\theta} \tag{1}$$

where φ is the air gap flux, R the reluctance by which the flux passes, and θ the rotor position.

Figure 2(a) illustrates a schematic diagram of magnet and pole pieces. Fig. 2(b) shows the reluctance variation and cogging torque waveform from **A** to **E** positions. The explanation of these waveforms is as follows: the d-axis for position **A** is directly under the center of the pole piece; this represents the stable position. Also, this position gives a minimum reluctance path for which the rate of change of the air gap reluctance ($\frac{dR}{d\theta}$) is zero, so the cogging torque is zero. For position **B**, the d-axis is directly under the position bisecting the pole piece and the slot; from position **A** to **B**, the reluctance value is increased, so $\frac{dR}{d\theta}$ has a positive sign giving a maximum negative cogging torque, which makes the rotor tend to return to the stable position. Position **C** is an unstable position because any slight disturbance will create torque to roll the rotor to the nearest pole piece; the d-axis is positioned at the center of the slot through which the reluctance is at maximum value; furthermore, $\frac{dR}{d\theta}$ is zero, hence, no cogging torque. From position **C** to **D**, $\frac{dR}{d\theta}$ is gradually decreasing, which will generate a maximum positive cogging torque at position **D**. Finally, if the d-axis is located at **E**, the rotor realizes one cogging torque period T, where this is the stable position for which the cogging torque is zero. The operation of these five cases will be repeated periodically if the rotor continuously rotates [25].

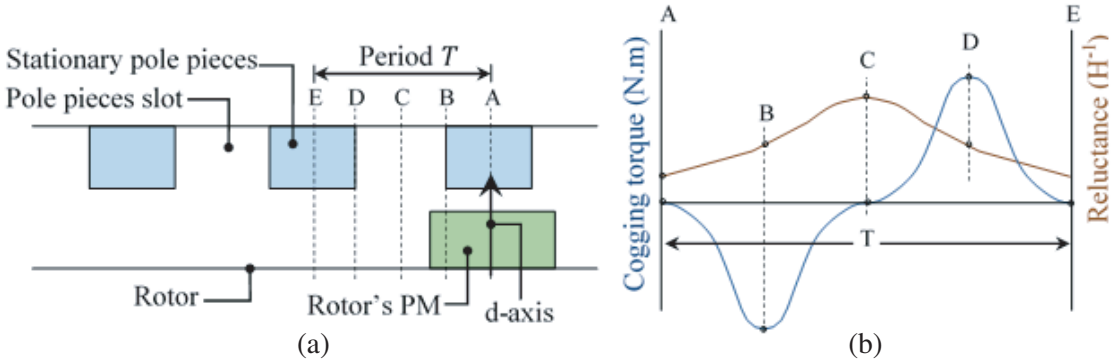

Figure 2. Reluctance and cogging torque variations. (a) Pole pieces/magnet arrangement. (b) Reluctance and cogging torque waveforms.

[26] has proposed and analyzed an MG illustrated in Fig. 3. This MG will be taken as a case of study, and the parameters of this MG are described in Table 1.

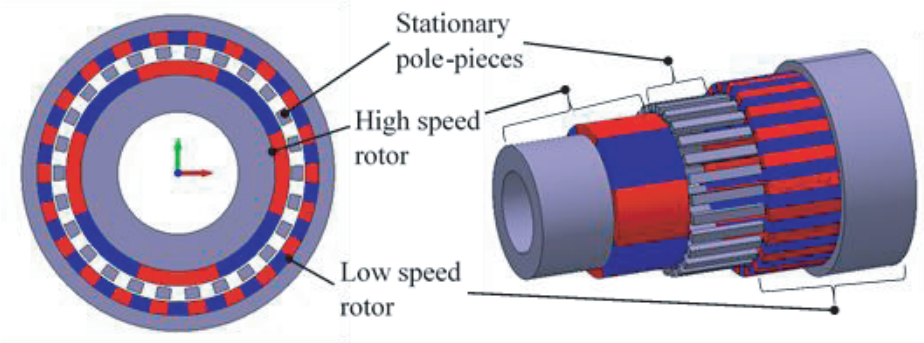

Figure 3. The selected MG.

Table 1. Parameters of the MG.

Description	Value
Pole-pairs number of high-speed rotor	4
Pole-pairs number of low-speed rotor	22
Number of ferromagnetic pole-pieces	26
Inner rotor back iron radius	43.5 mm
Inner rotor back iron thickness	16.5 mm
Inner rotor PMs radial thickness	5 mm
Outer rotor back iron radius	70 mm
Outer rotor back iron thickness	7 mm
Outer rotor PMs radial thickness	5 mm
Air gap radial thickness	1 mm
Pole-pieces radial thickness	5 mm
Permeance of flux density	1.26 T
Silicon steel type	M-19

Zhu and Howe in [27] introduced the cogging torque factor C_f through which they studied how the slot/pole combination of PM machines affects the cogging torque. This factor can be calculated as in (2), where LCM is the least common multiple, $2p$ the number of pole-pairs, and n_s the number of pole-pieces. Therefore, for the selected MG, $C_f = 2$.

$$C_f = \frac{2p * n_s}{LCM(2p, n_{s)}} \tag{2}$$

3. COGGING TORQUE MINIMIZATION METHOD

In this section, the slicing method will be used to mitigate the cogging torque. This method is based on dividing the rotors of MG into n number of slices. Furthermore, each slice is shifted angularly by an appropriate angle α, viz. for $(n = 3)$ model, the second slice is shifted from the first slice by α, while the third slice is shifted from the first slice by 2α making the d-axis of each magnet align with a pole piece at a different position. So, the resulting cogging torque is the vector sum of cogging torque of all slices through which the magnitude is dramatically reduced.

The cogging torque period θ in mechanical degree is defined as in (3) [28]:

$$\theta = \frac{360^\circ}{LCM(2p, n_s)} \tag{3}$$

Using (3), the cogging torque period for the high-speed rotor (HSR), (θ_{in}), is 3.46°, and for the low-speed rotor (LSR), the cogging torque period (θ_{out}) is 0.629°. For n number of slices, each slice must be rotated by α, where $\alpha = \frac{\theta}{n};\ n > 1$.

If the outer rotor is rotated by α, the inner rotor must be rotated by $(G_{hl} \times \alpha)$ to maintain synchronism between the two rotors, where G_{hl} is the gear ratio of the MG, which is calculated in [26] and equals -5.5. Fig. 4(a) and Fig. 4(b) show a schematic example of an MG with $(2p = 6)$ on the outer rotor and $(2p = 4)$ on the inner rotor and their corresponding cogging torque waveforms.

If the axial length (z-axis) of both rotors of the MG is divided into three slices $(n = 3)$ and each slice rotated by α, the total cogging torque will be eliminated, where δ represents the angle of circumferential direction. The schematic diagram of these slices and the related cogging torque waveforms are shown in Fig. 4(c) and Fig. 4(d). Because the rotors are equally sliced, the cogging torque magnitude is the same for all slices, so the only d-axis of each waveform is shifted by α. Therefore, the waveform of total cogging torque is reduced significantly on both rotors.

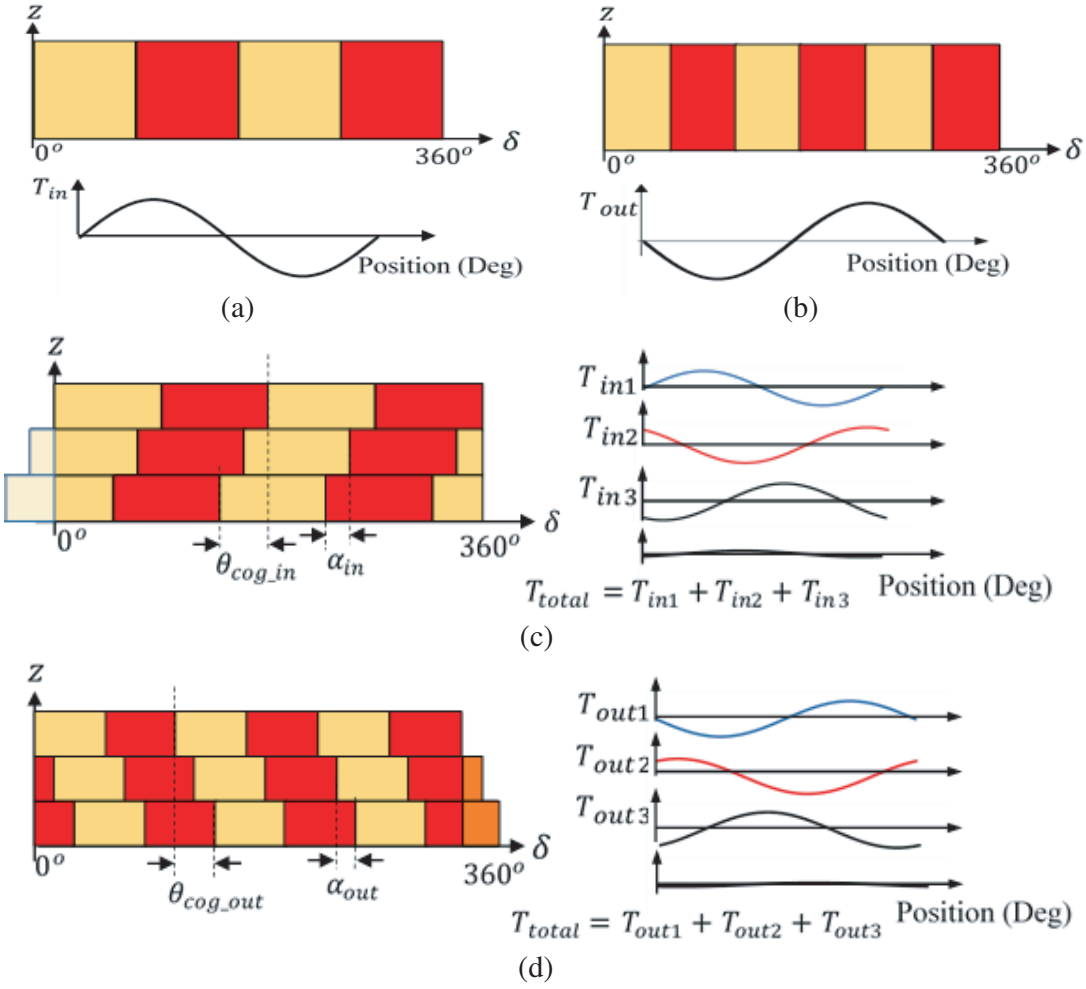

Figure 4. Cogging torque waveforms. (a) The inner rotor of the unsliced model. (b) The outer rotor of the unsliced model. (c) Inner rotor with three slices. (d) Outer rotor with three slices.

For the selected MG of [26], different numbers of slices will be applied in order to verify the method and evaluate the optimal model for cogging torque mitigation.

4. EVALUATION BY FE

In order to solve and analyze the MG, the mechanism must be defined, viz., which part of the MG will be the rotor and which one will be the stator. For the selected MG, the pole pieces are considered to be stationary, and the HSR and LSR are rotated in opposite directions because of a negative gear ratio (-5.5). The method used for predicting the T_{cog} on both rotors will be evaluated using a *2D static solver*, where the rotors are rotated in steps, and for each step, T_{cog} is determined. The accuracy of this method is based on the number of steps per cycle of T_{cog}. Then, the MG will be solved using *transient 2D with motion solver* for the load conditions. Different models with different numbers of slices have been investigated in this work as illustrated in Fig. 5. Each slice in a single model has been constructed and solved separately in the same time domain. MATLAB software is linked to Simcenter software to facilitate the process of evaluation of the models. The resultant torque of the model (cogging torque, torque ripple, and mean torque) is equal to the vector sum of all slices results.

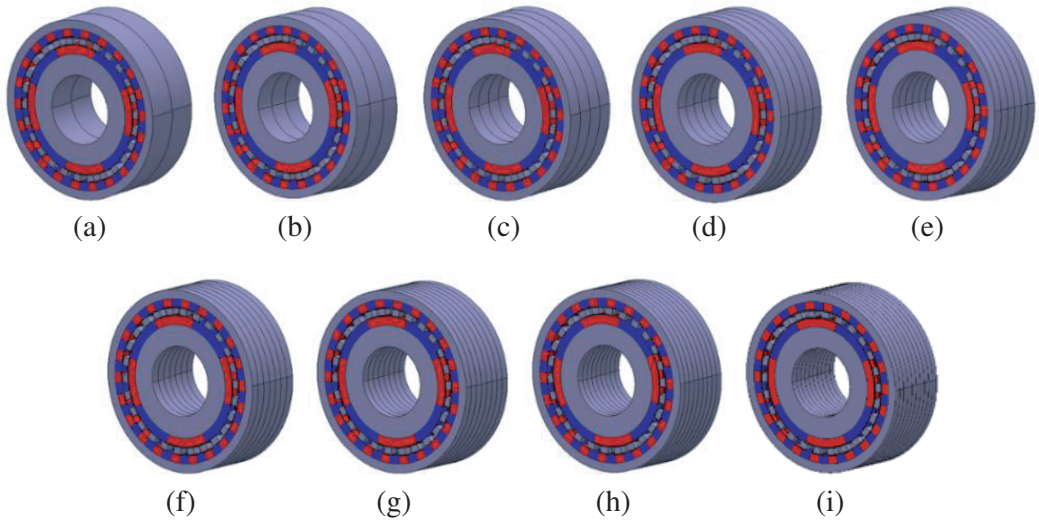

Figure 5. Slicing models for the selected MG. (a) $n = 2$. (b) $n = 3$. (c) $n = 4$. (d) $n = 5$. (e) $n = 6$. (f) $n = 7$. (g) $n = 8$. (h) $n = 9$. (i) $n = 10$.

5. RESULTS AND DISCUSSIONS

First of all, in order to validate the accuracy of the original model [26] and the proposed models, the original model has been analyzed by 2D FEM for maximum torque angle on the outer rotor ($\varphi = 4.09°mech$), and the maximum torque densities of both rotors are verified according to [26]. The torque density is the volumetric torque density (Nm/m^3). Since the diameter of the MG is constant, the surface area is also constant. So in this work, the torque density will be taken as the torque per axial length unit (Nm/m).

The fundamental component of the cogging torque for HSR is (104) and for LSR is (572). Therefore, the most effective cogging torque belongs to the HSR. The results of the original model are shown in Table 2. Table 3 shows the values of the angle α through which both rotors should rotate for each proposed model; note that $n = 1$ is for the original model. The comparison between the values of the maximum torque density, cogging torque, and torque ripple for the original and proposed models is shown in Fig. 6.

Table 2. The results of the original model.

Description	HSR	LSR
Cogging torque, (Nm)	0.986	0.109
Torque ripple (Nm)	0.831	0.07
Maximum torque density, (Nm/m)	332.42	1822.2

Table 3. The values of slicing angles for each model.

No. of slices n		2	3	4	5	6	7	8	9	10
α (Deg)	HSR	1.73	1.15	0.87	0.69	0.58	0.49	0.43	0.38	0.35
	LSR	−0.31	−0.21	−0.16	−0.13	−0.10	−0.09	−0.08	−0.07	−0.06

As evident in Fig. 6(a) and Fig. 6(b), the torque density has improved on both rotors; in Fig. 6(c) and Fig. 6(d), the torque ripple has minimized, which means that the cogging torque has been eliminated by the proposed models as shown in Fig. 6(e) and Fig. 6(f). As predicted in the literature, the slicing

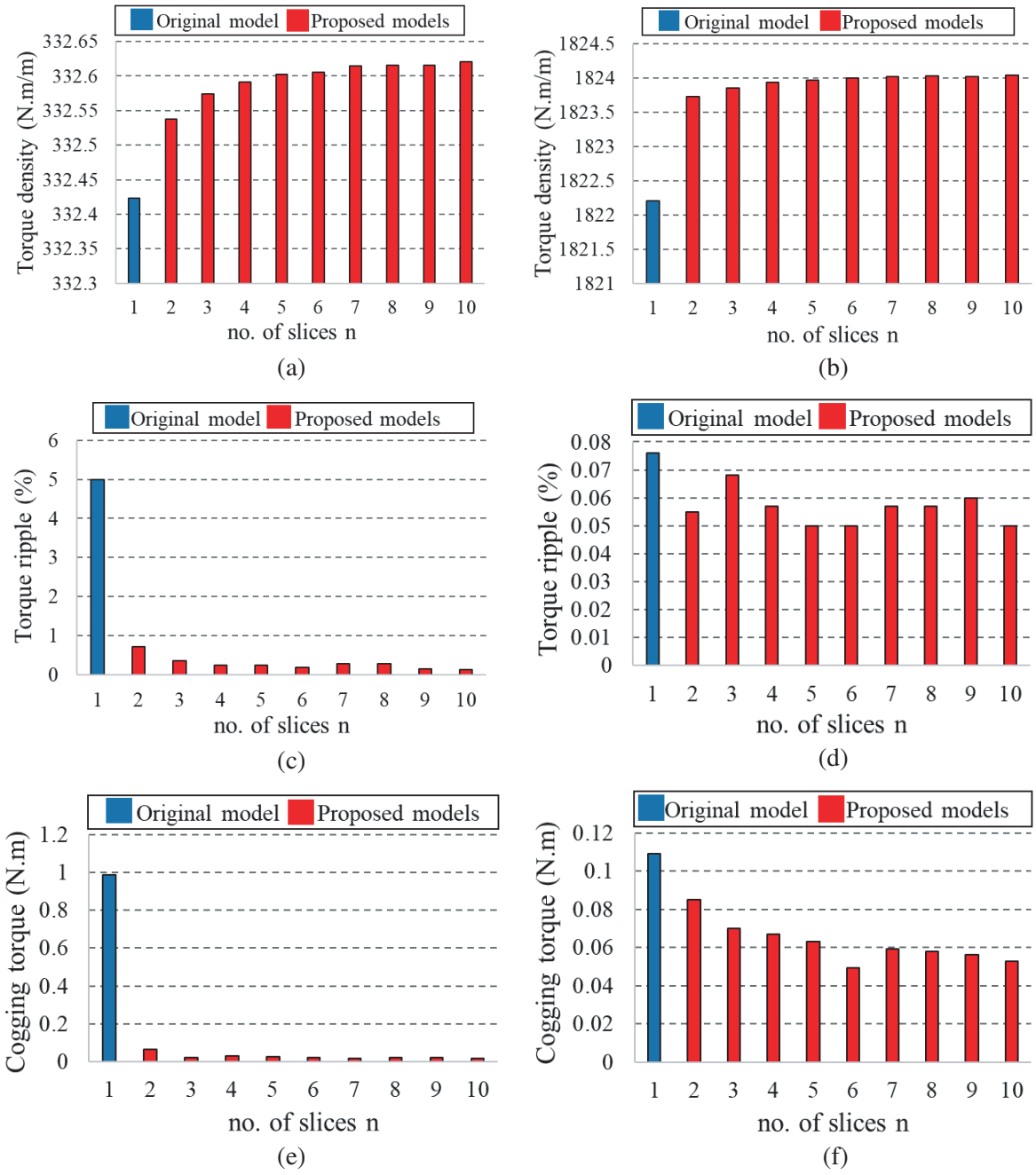

Figure 6. Comparison of the torque values of all models. (a) Torque density of the HSR. (b) Torque density of the LSR. (c) Percentage torque ripple of the HSR. (d) Percentage torque ripple of the LSR. (e) Cogging torque of the HSR. (f) Cogging torque of the LSR.

technique has a positive effect on the cogging torque, torque ripple, and the torque density.

The proper selection of the proposed MG requires some factors to be considered, such as design complexity, cogging torque, torque ripple, and the average torque. To achieve the goal of an optimal number of slices, a factor β has been introduced and considered as an objective function of maximum average torque (T_{avg}) and minimum torque ripple (T_r), where β can be defined as:

$$\beta = \frac{T_{avg}}{T_r} \tag{4}$$

As β is large, the torque ripple is minimum. Fig. 7 shows the variation of β as a function of slice number n for both rotors. It can be seen that all slicing models reduce the torque ripple, so according to Fig. 7(a), the factor β has an optimal point at $n = 10$, while in Fig. 7(b), β has three optimal points.

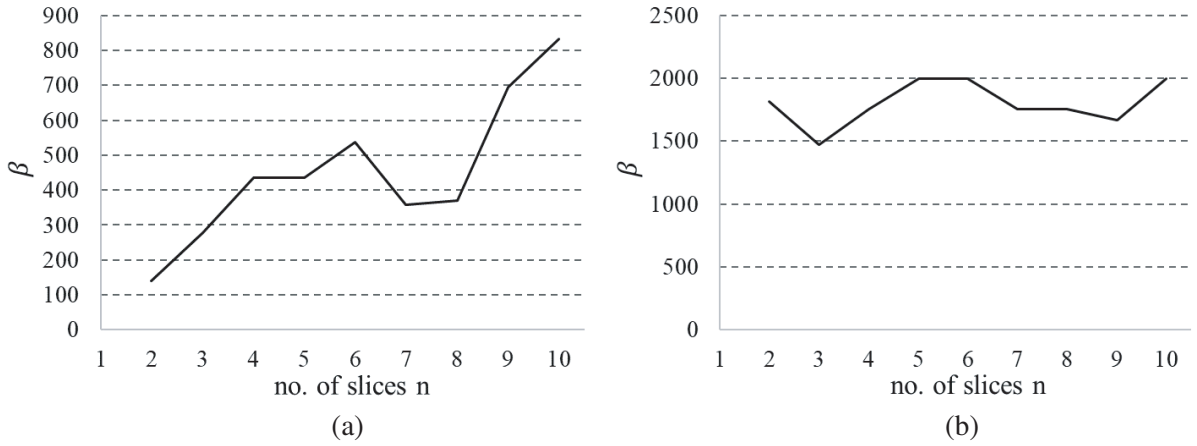

Figure 7. Torque to ripple ratio of the proposed models. (a) HSR. (b) LSR.

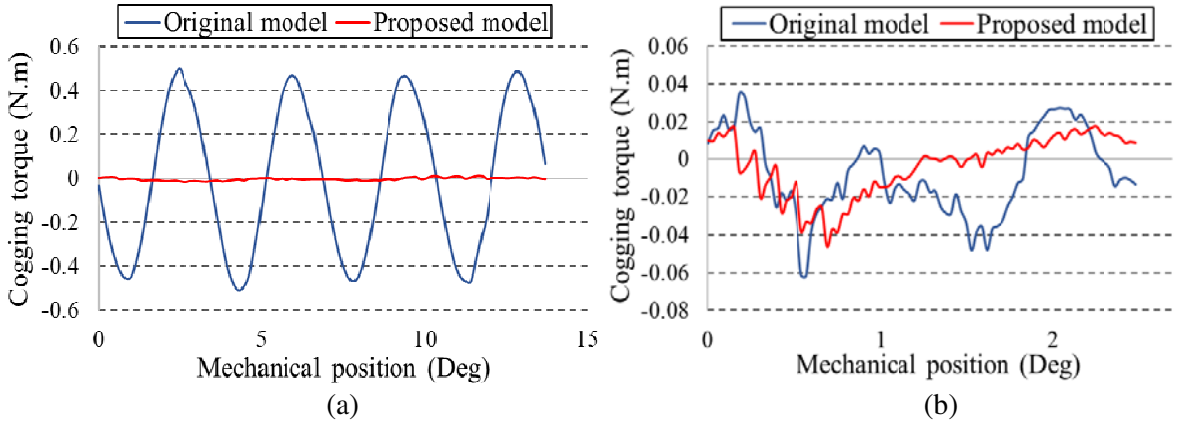

Figure 8. Cogging torque of the original and proposed model. (a) HSR. (b) LSR.

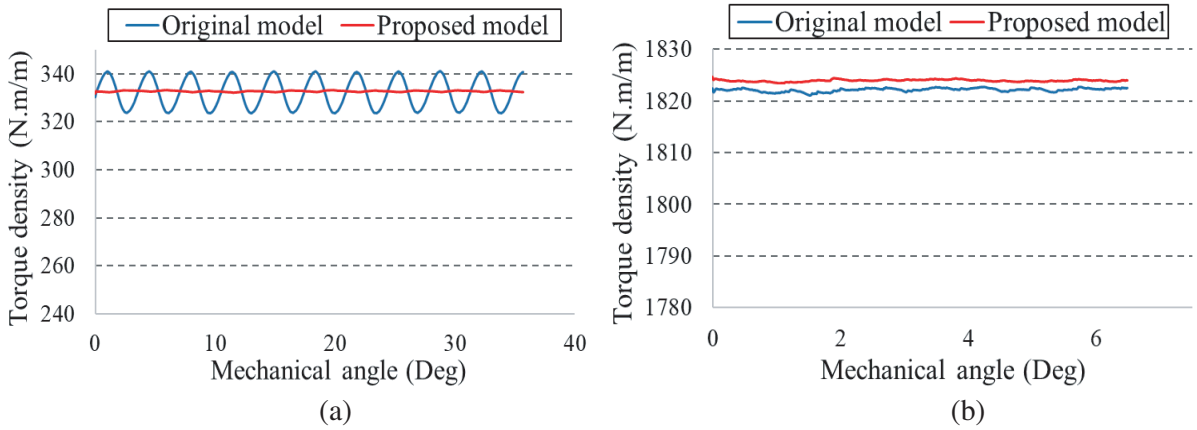

Figure 9. Torque density of the original and proposed model. (a) HSR. (b) LSR.

However, from the design complexity point of view, the optimal number of slices is 5. The summary of the results is shown in Table 4. Fig. 8 shows the waveforms of cogging torques for the original and optimized models. Furthermore, the LSR has a small reduction of cogging torque because the cogging torque in the original model is initially small but also decreased by this method. The torque densities of the two models are shown in Fig. 9; there is a slight improvement in the torque density on both rotors. Hence, from the results, the torque ripple that existed clearly in the inner torque density of the original model has been canceled.

Table 4. Summary of the results.

Description	Original model	Proposed model	Percentage improvement (%)
Cogging torque of HSR, (Nm)	0.986	0.0243	97.53
Cogging torque of LSR, (Nm)	0.109	0.0629	42.3
Torque ripple of HSR (Nm)	0.831	0.0382	95.4
Torque ripple of LSR (Nm)	0.07	0.0456	34.8
Maximum torque density of HSR, (Nm/m)	332.42	332.6	0.05
Maximum torque density of LSR, (Nm/m)	1822.2	1824	0.1

6. CONCLUSIONS

This paper has proposed a rotor slicing technique as a cogging torque reduction method in MGs. Slicing both rotors of the MG was very efficient compared with the slicing of one rotor, described in the literature. Thanks to this technique, the cogging torque has been dramatically eliminated on both rotors, and the overall performance of the MG has been improved. It is obvious that the cogging torque elimination is increased directly with the number of slices, but the cost and manufacturing complexity are also increased. It has been recognized that the factor β played a significant role in the selection of the optimal number of slices combined with FE sensitivity analysis. Finally, this method can be generalized for all PM machines with a high cogging torque factor C_f due to its principle of elimination. Therefore, if the MGs are ripple free, they can be used as substitutions for mechanical gears in applications requiring a precise position and smooth rotation, such as automobiles, mechanical clocks, elevators, and printing machines. Other applications of MGs are in the fields of marine energy, renewable energy systems, defense industry, and spacecraft.

REFERENCES

1. Jian, L., K. Chau, and J. Jiang, "An integrated magnetic-geared permanent-magnet in-wheel motor drive for electric vehicles," *2008 IEEE Vehicle Power and Propulsion Conference*, 1–6, IEEE, 2008.
2. Rens, J., K. Atallah, S. D. Calverley, and D. Howe, "A novel magnetic harmonic gear," *IEEE Transactions on Industry Applications*, Vol. 46, No. 1, 206–212, 2009.
3. Huang, C.-C., M.-C. Tsai, D. G. Dorrell, and B.-J. Lin, "Development of a magnetic planetary gearbox," *IEEE Transactions on Magnetics*, Vol. 44, No. 3, 403–412, 2008.
4. Atallah, K. and D. Howe, "A novel high-performance magnetic gear," *IEEE Transactions on Magnetics*, Vol. 37, No. 4, 2844–2846, 2001.
5. Neves, C. G., Á. Flores, D. L. Figueiredo, and A. S. Nunes, "Magnetic gear: A review," *2014 11th IEEE/IAS International Conference on Industry Applications*, 1–6, IEEE, 2014.

6. Dosiek, L. and P. Pillay, "Cogging torque reduction in permanent magnet machines," *IEEE Transactions on Industry Applications*, Vol. 43, No. 6, 1565–1571, 2007.
7. Gerber, S. and R.-J. Wang, "Cogging torque definitions for magnetic gears and magnetically geared electrical machines," *IEEE Transactions on Magnetics*, Vol. 54, No. 4, 1–9, 2018.
8. Jungmayr, G., J. Loeffler, B. Winter, F. Jeske, and W. Amrhein, "Magnetic gear: Radial force, cogging torque, skewing, and optimization," *IEEE Transactions on Industry Applications*, Vol. 52, No. 5, 3822–3830, 2016.
9. Bekhouche, L., R. Saou, A. K. Cherif Guerroudj, and M. E.-H. Zaim, "Electromagnetic torque ripple minimization of slotted doubly-salient-permanent-magnet generator for wind turbine applications," *Progress In Electromagnetics Research M*, Vol. 83, 181–190, 2019.
10. Jing, L., Z. Huang, J. Chen, and R. Qu, "Design, analysis, and realization of a hybrid-excited magnetic gear during overload," *IEEE Transactions on Industry Applications*, Vol. 56, No. 5, 4812–4819, 2020.
11. Jing, L., Z. Huang, J. Chen, and R. Qu, "An asymmetric pole coaxial magnetic gear with unequal Halbach arrays and spoke structure," *IEEE Transactions on Applied Superconductivity*, Vol. 30, No. 4, 1–5, 2019.
12. Caruso, M., A. O. Di Tommaso, R. Miceli, and F. Viola, "A cogging torque minimization procedure for interior permanent magnet synchronous motors based on a progressive modification of the rotor lamination geometry," *Energies*, Vol. 15, No. 14, 4956, 2022.
13. Hüner, E. and G. Zeka, "Reduction of cogging torque and improvement of electrical parameters in Axial Flux Permanent Magnet (AFPM) synchronous generator with experimental verification," *Progress In Electromagnetics Research C*, Vol. 104, 99–113, 2020.
14. Taghipour Boroujeni, S. and V. Zamani, "Influence of magnet shaping on cogging torque of surface-mounted PM machines," *International Journal of Numerical Modelling: Electronic Networks, Devices and Fields*, Vol. 29, No. 5, 859–872, 2016.
15. Zamani Faradonbeh, V., S. Taghipour Boroujeni, and N. Takorabet, "Optimum arrangement of PMs in surface-mounted PM machines: Cogging torque and flux density harmonics," *Electrical Engineering*, Vol. 102, No. 3, 1117–1127, 2020.
16. Huang, X., Y. Guo, and L. Jing, "Comparative analysis of electromagnetic performance of magnetic gear," *Progress In Electromagnetics Research Letters*, Vol. 97, 69–76, 2021.
17. Taghipour Boroujeni, S., N. Takorabet, S. Mezani, T. Lubin, and P. Haghgooie, "Using and enhancing the cogging torque of PM machines in valve positioning applications," *IET Electric Power Applications*, Vol. 14, No. 12, 2516–2524, 2020.
18. Ge, X., Z. Zhu, G. Kemp, D. Moule, and C. Williams, "Optimal step-skew methods for cogging torque reduction accounting for three-dimensional effect of interior permanent magnet machines," *IEEE Transactions on Energy Conversion*, Vol. 32, No. 1, 222–232, 2016.
19. Washington, J. G., G. J. Atkinson, and N. J. Baker, "Reduction of cogging torque and EMF harmonics in modulated pole machines," *IEEE Transactions on Energy Conversion*, Vol. 31, No. 2, 759–768, 2016.
20. Song, Y., Z. Zhang, S. Yu, F. Zhang, and Y. Zhang, "Analysis and reduction of cogging torque in direct-drive external-rotor permanent magnet synchronous motor for belt conveyor application," *IET Electric Power Applications*, Vol. 15, No. 6, 668–680, 2021.
21. Wang, Y. and L. Jing, "A new structure for the coaxial magnetic gear with HTS bulks for fitness car," *Progress In Electromagnetics Research Letters*, Vol. 103, 39–48, 2022.
22. García-Gracia, M., A. Jimenez Romero, J. Herrero Ciudad, and S. Martin Arroyo, "Cogging torque reduction based on a new pre-slot technique for a small wind generator," *Energies*, Vol. 11, No. 11, 3219, 2018.
23. Hwang, M.-H., H.-S. Lee, and H.-R. Cha, "Analysis of torque ripple and cogging torque reduction in electric vehicle traction platform applying rotor notched design," *Energies*, Vol. 11, No. 11, 3053, 2018.

24. Kwon, J.-W., J.-H. Lee, W. Zhao, and B.-I. Kwon, "Flux-switching permanent magnet machine with phase-group concentrated-coil windings and cogging torque reduction technique," *Energies*, Vol. 11, No. 10, 2758, 2018.
25. Jiang, J. W., B. Bilgin, Y. Yang, A. Sathyan, H. Dadkhah, and A. Emadi, "Rotor skew pattern design and optimisation for cogging torque reduction," *IET Electrical Systems in Transportation*, Vol. 6, No. 2, 126–135, 2016.
26. Atallah, K., S. D. Calverley, and D. Howe, "Design, analysis and realisation of a high-performance magnetic gear," *IEE Proceedings — Electric Power Applications*, Vol. 151, 135–143, 2004.
27. Zhu, Z. and D. Howe, "Influence of design parameters on cogging torque in permanent magnet machines,"*IEEE Transactions on Energy Conversion*, Vol. 15, No. 4, 407–412, 2000.
28. Hsiao, C.-Y., S.-N. Yeh, and J.-C. Hwang, "A novel cogging torque simulation method for permanent-magnet synchronous machines," *Energies*, Vol. 4, No. 12, 2166–2179, 2011.